We are IntechOpen, the world's leading publisher of Open Access books Built by scientists, for scientists

4,800
Open access books available

122,000
International authors and editors

135M
Downloads

Our authors are among the

154
Countries delivered to

TOP 1%
most cited scientists

12.2%
Contributors from top 500 universities

CLARIVATE ANALYTICS BOOK CITATION INDEX INDEXED

WEB OF SCIENCE™

Selection of our books indexed in the Book Citation Index in Web of Science™ Core Collection (BKCI)

Interested in publishing with us?
Contact book.department@intechopen.com

Numbers displayed above are based on latest data collected.
For more information visit www.intechopen.com

9

Performance Of Microturbine Generation System in Grid Connected and Islanding Modes of Operation

Dattatraya N. Gaonkar
National Institute of Technology Karnataka Surathkal
India

1. Introduction

The distributed generation system based on microturbine technology is becoming more potential and viable distributed energy source in the recent years. This is due to their salient features such as high operating efficiency, ultra low emission levels, low initial cost and small size (Scott, 1998 and Gaonkar, 2006). The microturbine generation system (MTG) produce power in the range of 25-500 kW and can be operated in stationary or mobile, remote or interconnected with the utility grid. Once connected to power distribution system, these generators will affects the dynamics of the system. Hence dynamic models are necessary to deal with issues in system planning, interconnected operation and management. There is lack of adequate information on the performance of MTG system when connected to distribution network, even though microturbine is based on gas turbine technology, which is well established (Scott, 1998 and Al-Hinai, 2002). In particular, little development has been made on the effective modeling of these DG systems. The design of power electronic converter interface, needed for single shaft MTG system presents a significant challenge (Nikkhajoei, 2005 and Illanda, 2002). The dynamic models of MTG system for isolated operations are reported in (Al-Hinai, 2002, Gaonkar, 2006 and Guda, 2004). But in these works only isolated operation of MTG system is considered. The grid connected model of MTG system with various power electronic topologies are reported in (Azmy, 2003, Fethi, 2004 and Nikkhajoei 2005). These topologies have there own disadvantages which over come by the back to back converter topologies.

One of the important technical issues created by DG interconnection to the utility is the islanding of DG units (Villeneuve, 2004). This mode of DG operation is encouraged by the ongoing rapid development of new generation technologies such as micro-turbines, wind generators, fuel cells, photovoltaic plants and their increased penetration in the utility network. Furthermore, the remarkable improvements in the power electronic technology make it possible to design seamless scheme for transferring DG operation between grid connected and islanding modes without interruption in the power supply [Barsali, 2002]. The intentional islanding mode operation is utmost important in the case of sensitive and mission-critical industrial loads as there is a need to maintain a continuous and uninterrupted AC power during planned or unplanned grid outage conditions (Tirumala ,

2002 and Illanda, 2002). The IEEE Std. 1547-2003 states the need for implementing intentional islanding operation of DG systems (IEEE, 2003). As a consequence, research in the last few years has been motivated to study the possibility of intentional islanding of various DG systems.
In the above context this chapter presents the technology, application and performance study of the micro turbine generation system. The detailed modeling of a single-shaft MTG system suitable for grid connection in Simulink of the Matlab is given in this chapter. The algorithm for seamless transfer of microturbne generation system operation between grid connected and islanding mode is presented in this chapter.

2. Types of Microturbine Design

The basic components of a microturbine are the compressor, combustor, turbine generator and recuperator. It operates on the same principles as traditional gas turbines. Air is drawn into the compressor, where it is pressurized and forced into the cold side of the recuperator. Here, exhaust heat is used to preheat the air before it enters the combustion chamber. The combustion chamber then mixes the heated air with fuel and burns it. This mixture expands through the turbine, which drives the compressor and generator.
There are two types of micro turbine designs available, based on position of compressor turbine and generator. Figure 1 (a) shows a high speed single shaft design with the compressor and turbine mounted on the same shaft along with the permanent magnet synchronous generator. The generator generates power at very high frequency ranging from 1500 to 4000 Hz. The high frequency voltage is first rectified and then inverted to a normal AC power at 50 or 60 Hz. Another design is shown in Fig. 1 (b) in which the turbine on the first shaft directly drives the compressor while a power turbine on the second shaft drives the gearbox and conventional electrical generator (usually induction generator) producing 60 Hz power. The two-shaft design features more moving parts but does not require complicated power electronics to convert high frequency AC power output to 60 Hz.

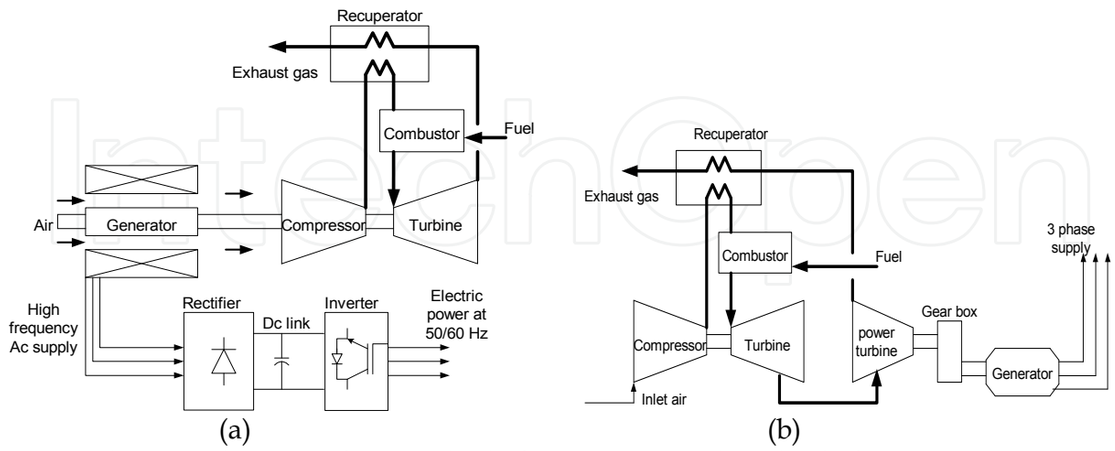

Fig. 1. Schematic diagram of (a) single shaft MTG system (b) split shaft MTG system

Microturbine turbo-machinery is based on single-stage radial flow compressors and turbines. This offers highest efficiency in various size ranges; where as moderate to large

size gas turbines use multi-stage axial flow turbines and compressors. In a microturbine, the turbo-compressor shaft generally turns at high rotational speed as high as 1, 20,000 rpm based on the power rating. The microturbine utilizes gas foil bearings (air bearings) for high reliability, low maintenance and safe operation. This needs minimum components and no liquid lubrication is necessary to support the rotating group. Recuperators are heat exchangers that use the hot exhaust gas of the turbine (typically around 1,200ºF) to preheat the compressed air (typically around 300ºF) going into the combustor. This reduces the fuel needed to heat the compressed air to turbine inlet temperature. With recuperator microturbine efficiency can go above 80%.

3. Power Electronic Interface Topologies

The single shaft MTG system is widely used for power generation applications rather than split shaft due its advantages. As discussed, single shaft microturbine design requires power electronic converter interface to convert the high frequency AC power produced by the generator into usable electricity. This is a critical component in the single shaft microturbine design. It represents significant design challenges, specifically in matching turbine output to the required load. Generally, power electronic interface circuits are designed to with stand transients and voltage spikes up to seven times the nominal voltage.

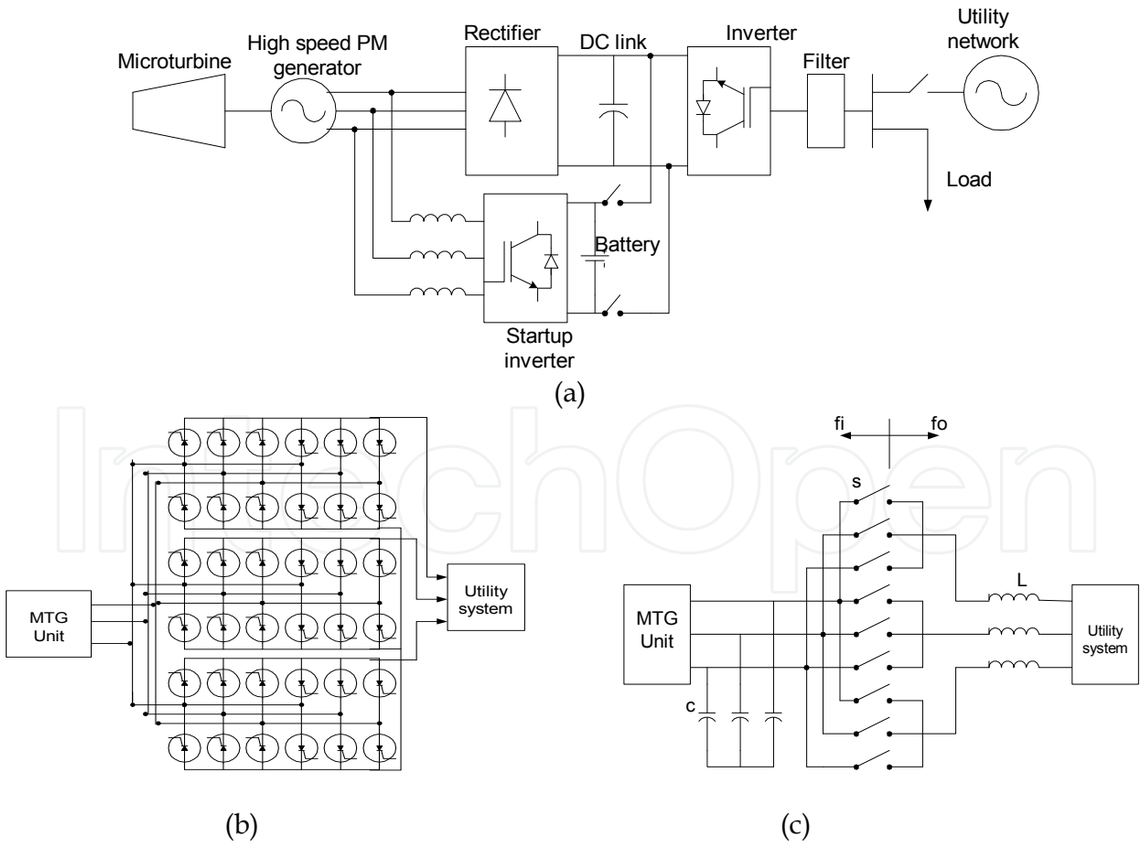

Fig. 2. (a) Passive rectifier and inverter combination (b) Cycloconverter interface model (c) Matrix converter interface model.

There are different interface topologies available for connecting single shaft MTG systems to grid. Figure 2 (a) shows the passive rectifier and inverter combination with DC link. This design needs separate startup inverter for motoring operation of generator to launch the microturbine and also during cool-down process, to remove heat stored in the recuperator and microturbine engine, in order to protect the system components. A cycloconverter and matrix converter shown in Fig. 2 (b) and Fig. 2 (c) can be used to interface the microturbine generator to the grid (Azmy, 2003 and Nikkhajoei 2005). These converters directly convert AC voltages at one frequency to AC voltages at another frequency with variable magnitude. For this reason, they are also called frequency changers. The disadvantages of these converters are that they have double the number of switches compared to the DC link approach and energy storage is not possible. If there is no DC link, any fluctuation on either side of the converter will directly influence the other side.
The matrix converter shown in Fig.2 (c) can be used at lower frequency compared to PWM based converters. Some advantages of the matrix converters are less thermal stress on the semiconductors during low output frequency and absence of the DC link capacitors which increases the efficiency and life time. The drawbacks of this topology are the intrinsic limitation of the output voltage, the unavailability of a true bi-directional switch; absence of decoupling between the input and the output of the converter. This may lead to some instability issues (Teodorescu, 2004). The back to back voltage source converters (VSC) interface topology is shown in Fig. 3. This topology allows bi-directional power flow between the converter and the grid and hence no separate starting arrangement is required. At the time of starting, permanent magnet synchronous machine acts as motor and draws power from the grid to bring the turbine to certain speed. During the generating mode PMSM acts as generator and power flows from MTG system to grid (Fethi, 2004 and Gaonkar, 2008).

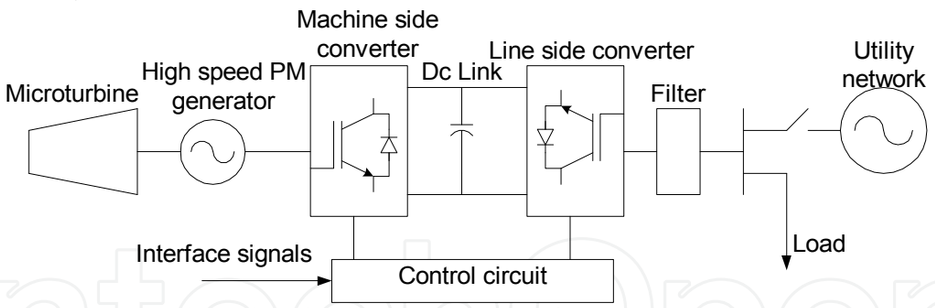

Fig. 3. MTG system with back to back converter interface

4. Applications of MTG System

Microturbine generation system can be used for a wide range of applications. Some of the applications are discussed in this section (Scott, 1998).

4.1 Base load, peak shaving and stand-alone power

Microturbine based DG system can operate in parallel with grid or with any other generation source. The microturbine can augment utility supply during peak load periods, thus increasing power reliability and reducing or eliminating peak demand charges. Shaving peaks will increase overall system efficiency which will reduce investments in

traditional generation, bulk transmission, and distribution facilities. Shaving peaks will also enable the utility to serve incremental load growth in areas where there is a shortage of substation and/or distribution feeder capacity. The Microturbine can provide prime power generation where the electric utility grid is not readily available or where service is unreliable.

4.2 Combined Heat and Power

Cogeneration, or combined heat and power (CHP) generation refers to the process of utilizing the heat produced by a combustion engine as energy output. During normal operation, microturbine produces significant quantities of high-temperature exhaust that can be easily integrated with a heat exchanger and a hot water loop to produce valuable energy output. From a cost-benefit perspective, this yields a significant saving compared to heating fuel and purchasing power. When the heat energy is utilized, overall system fuel efficiency can range between 70 and 90+%.

4.3 Resource Recovery

Flared gases often have low-energy yield or high contents of corrosive "sour" (hydrogen sulphide, or H_2S) gas, making them an infeasible fuel source for conventional generators. Microturbine, on the other hand has no problem operating exclusively on low-energy gases. Microturbine can also be used in oil and gas recovery applications. With the ability to convert unprocessed casing gas that contains up to 7% corrosive H_2S gas, microturbine can eliminate the need for flaring. At the same time, their power output reduces or eliminates the need for additional electricity sources.

4.4 UPS and Stand by Services

The microturbine technology can be integrated into a wide variety of products and systems. Uninterruptible power supplies, all-in-one combined heat and power systems, and welding machines are just a few examples for original equipment manufacturing applications.

5. Modeling of MTG System Components

The integrated model of MTG system consists of microturbine, permanent magnet synchronous machine, machine and grid side converters with control and filter. The modeling of individual components is described in this section (Rowen, 1983).

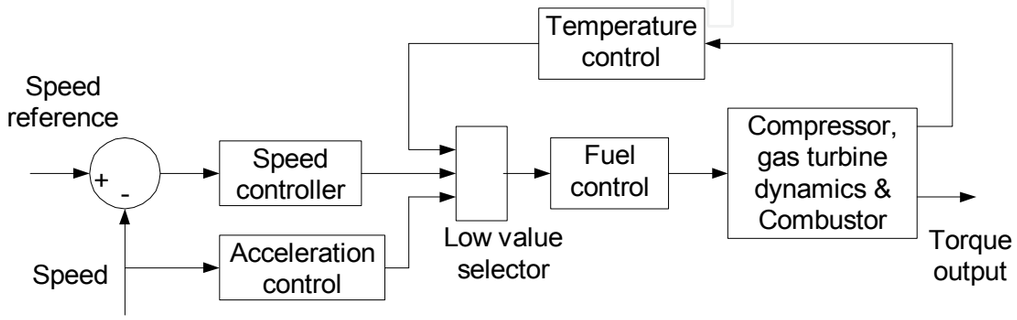

Fig. 4. Block diagram of microturbine system with controls

5.1 Microturbine

The block diagram of microturbine along with its control is shown in Fig. 4. This consists of fuel, speed, acceleration and temperature control along with the combustor and turbine dynamics. The implementation of microturbine model using Simulink of the Matlab is shown in Fig 5.

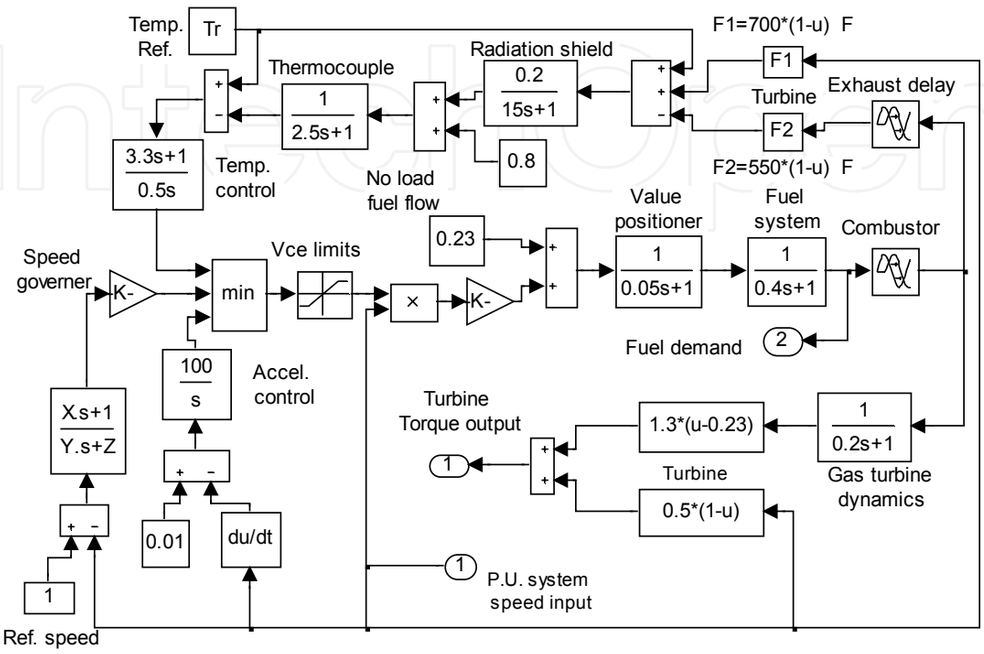

Fig. 5. Simulink model of the microturbine

Speed and acceleration control: The speed control operates on the speed error formed between a reference (one per-unit) speed and the rotor speed of the MTG system. It is the primary means of control for the microturbine under different load conditions. Speed control is usually modeled by using a lead-lag transfer function or by a PID controller (Hajagos, 2001).Acceleration control is used primarily during gas turbine startup to limit the rate of rotor acceleration prior to reaching governor speed. This ameliorates the thermal stress encountered during startup. Acceleration controller is an integrator as shown in Fig. 5 and acts on the error between the derivative of p. u. speed of generator and constant reference signal.

Temperature control: The temperature control is the common method of limiting gas turbine output at a predetermined firing temperature, independent of variation in ambient temperature or fuel characteristics. The fuel burned in the combustor results in turbine torque and in exhaust gas temperature. The exhaust gas temperature is measured using a series of thermocouples incorporating radiation shields. The thermocouples and radiation shields are represented by transfer functions as shown in Fig. 5.The output from the thermocouple is compared with a temperature reference value. Normally the reference value is higher than the thermocouple output. This forces the output from the temperature control to stay on the maximum limit permitting uninhibited governor/speed control. When the thermocouple output exceeds the reference temperature, the difference becomes

negative and it starts lowering the temperature control output. When the temperature control output becomes lower than the speed governor output, the former value will pass through the low value selector to limit the output and the unit will operate on temperature control (Rowen, 1983).

Fuel control: The outputs of the speed governor, acceleration controller and temperature control system go as input to a minimum value selector, which selects the lowest value among three inputs. The output of low value selector represents the least amount of fuel required for that particular operating point and is denoted as 'Vce'. The per unit value for 'Vce', corresponds directly to the per unit value of mechanical power on turbine base in steady state. The output of the low value selector is compared with maximum and minimum limits. The maximum limit acts as back up to temperature control and is not encountered in normal operation and minimum limit is more important dynamically. The out put of the 'Vce' limiter is multiplied by 0.77 and offset by no load fuel flow value to ensure the continuous combustion process. The fuel flow controls are represented by series of blocks including the valve position and flow dynamics.

Compressor, combustor and turbine: Turbine is a linear, non dynamic device with the exception of the rotor time constant. There is a small transport delay, which is the time lag associated with the compressor discharge volume. Another transport delay is due to the transport of gas from the combustion system through the turbine. The values of these delays are given in (Rowen, 1983 and Hajagos, 2001]. Both the torque and exhaust temperature characteristics of the single shaft gas turbines are essentially linear with respect to fuel flow and turbine speed. They are given by following equations.

$$\text{Turbine torque} = T = 1.3\,(w_{f2} - 0.23) + 0.5\,(1 - N) \tag{1}$$

$$\text{Exhaust gas temperature} = T_{ex} = T_R - 700\,(1 - w_{f1}) + 550\,(1 - N) \tag{2}$$

Where T_R is the reference temperature, N is per unit speed and W_f is per unit fuel demand signal. The constant value 1.3 in the turbine torque expression depends on the enthalpy or higher heating value of the gas stream in the combustion chamber. In this chapter microturbine is assumed to operate under normal operating conditions. Temperature control and acceleration control are of no significance under normal system conditions. They can be omitted in the turbine model. In this chapter electro-mechanical behavior of microturbine is our main interest. The recuperator is not included in the model as it is only a heat exchanger to raise the energy efficiency. Also due to the very slow response time of the recuperator, it has little influence on the timescale of dynamic simulations presented in this chapter. Thus microturbine model shown in Fig. 5 is simplified by using the above assumptions and resulted model is used in this investigation.

5.2 Permanent Magnet Synchronous Machine (PMSM)

The development of advanced magnetic materials, power electronics and digital control systems are making permanent magnet (PM) machine as an interesting solution for a wide range of applications. The advantages of PMSM compared to other AC machines are its simple structure, high-energy efficiency, reliable operation, high power density and possibility of super high speed operation. Recent important applications of permanent magnet synchronous machine are in the area of distributed generation, mainly in wind and

microturbine generation systems. An advantage of a high speed generator is that the size of the machine decreases almost in directly in proportion to the increase in speed, leading to a very small unit. Super high speed PMSM is an important component of single shaft MTG system. The mathematical model of a PMSM is similar to that of the wound rotor synchronous machine.

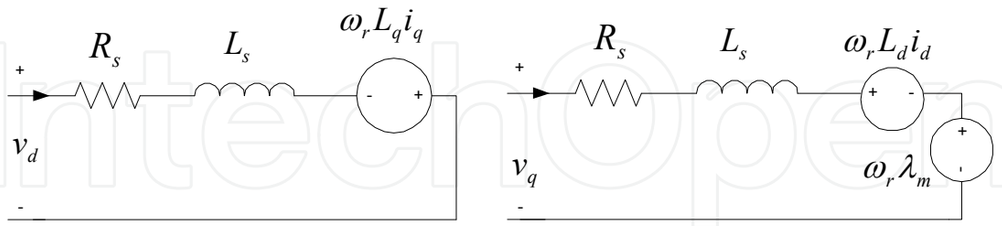

Fig. 6. *dq*-axis equivalent circuit model of the PMSM a) *d*-axis b) *q*-axis

The *dq*-axis equivalent circuit model of PMSM is shown in Fig. 6
The PMSM drive modeling is done with the assumption of sinusoidal distributed windings, saturation is neglected, **e**ddy currents and hysteresis losses are negligible (Pillai, 1989). With these assumptions the stator *dq* equations of the PMSM in the rotor reference frame are:

$$v_d = R_s i_d + L_d \frac{di_d}{dt} - p\omega_r L_q i_q \tag{3}$$

$$v_q = R_s i_q + L_q \frac{di_q}{dt} + p\omega_r L_d i_d + pw_r \Phi_m \tag{4}$$

Where, the stator resistance is denoted by R_s,, the *d*-axis and *q*-axis inductances are L_d and L_q respectively, Φ_m is the flux linkage due to the permanent magnets, v_d and v_q are *dq* axis voltages. In the *dq*-frame, the expression for electro-dynamic torque becomes:

$$T_e = 1.5p\,(\Phi_m i_q + (L_d - L_q) i_q i_d) \tag{5}$$

The equation for motor dynamics can be given as:

$$\frac{d}{dt}\omega_r = \frac{1}{J}(T_e - F\omega_r - T_M) \tag{6}$$

$$\frac{d}{dt}\theta_r = \omega_r \tag{7}$$

$$\begin{bmatrix} v_q \\ v_d \\ v_0 \end{bmatrix} = \frac{2}{3}\begin{bmatrix} \cos\theta_r & \cos(\theta_r - 120) & \cos(\theta_r + 120) \\ \sin\theta_r & \sin(\theta_r - 120) & \sin(\theta_r + 120) \\ 1/2 & 1/2 & 1/2 \end{bmatrix}\begin{bmatrix} v_a \\ v_b \\ v_c \end{bmatrix} \tag{8}$$

$$\begin{bmatrix} v_a \\ v_b \\ v_c \end{bmatrix} = \begin{bmatrix} \cos\theta_r & \sin\theta_r & 1 \\ \cos(\theta_r - 120) & \sin(\theta_r - 120) & 1 \\ \cos(\theta_r + 120) & \sin(\theta_r + 120) & 1 \end{bmatrix}\begin{bmatrix} v_q \\ v_d \\ v_0 \end{bmatrix} \tag{9}$$

Where p is the number of pole pairs, T_e is the electromagnetic torque, F is combined viscous friction of rotor and load, ω_r is the rotor speed, and J is the moment of inertia, θ_r is rotor angular position and T_m is shaft mechanical torque. The d, q variables are obtained from a, b, c variables through the Park transform given in (8) and a, b, c variables are obtained from the d, q variables through the inverse of the Park transform given in (9).

5.3 Machine Side Converter Control

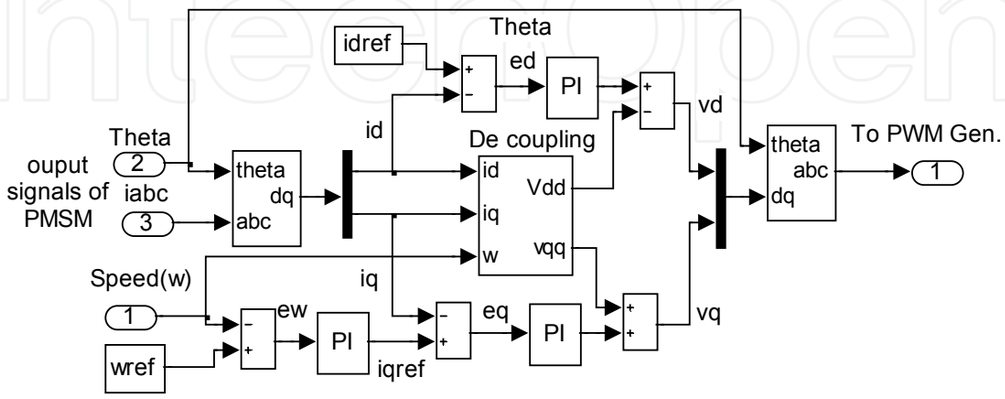

Fig. 7. Machine side converter controller implemented in Simulink

Figure 7 shows the Machine side converter controller implemented in Simulink of the Matlab. The commanded speed ω_{ref} is pre-calculated according to the turbine output power and set to the optimum speed (Morimoto, 1994 and Fethi, 2004). Based on the speed error the commanded q axis reference current iq_{ref} is determined through the speed controller. In this system the following PI controller is employed as the speed controller.

$$i_{qref} = K_{p\omega} e_{\omega} + K_{i\omega} \int e_{\omega} dt \tag{10}$$

Where, $K_{P\omega}$ and $K_{I\omega}$ are the proportional and integral gains of the speed controller respectively while, e_{ω} is the error between the reference speed and measured speed. The commanded optimal d-axis current i_{dref} is obtained from the maximum allowed phase voltage and phase current constraints of the drive, which are given in (11) and (12). These constraints depend upon the machine rating and DC link voltage.

$$v_d^2 + v_q^2 \le V_{\max}^2 \tag{11}$$

$$i_d^2 + i_q^2 \le I_{\max}^2 \tag{12}$$

Using the above constraints and neglecting the voltage drop due to the stator resistance, the optimal d-axis current for a non salient PMSM (L_d=L_q) can be obtained as:

$$I_d = \frac{\frac{V_{\max}^2}{\omega^2} - L_q^2 I_{\max}^2 - \lambda_m^2}{2 L_d \lambda_m} \tag{13}$$

Considering the relationship $I_{\max}^2 = i_d^2 + i_q^2$ the optimal d-axis current can be given as a function of the q-axis current i_q, as :

$$i_d = -\frac{\lambda_m}{L_d} + \sqrt{\left(\frac{V_{\max}}{\omega L_d}\right)^2 - (\frac{L_q}{L_d} i_q)^2} \tag{14}$$

Based on the current errors the d-*q* axis reference voltages are determined by PI controllers, as given in (15) and (16).

$$v_d = K_{Pi} e_{id} + K_{Ii} \int e_{id} dt - \omega_r L_q i_q \tag{15}$$

$$v_q = K_{Pi} e_{iq} + K_{Ii} \int e_{iq} dt + \omega_r (L_d i_d + \lambda_m) \tag{16}$$

Where, K_{Pi} and K_{Ii} are the proportional and integral gains of the controller respectively. $e_{id} = i_{dref} - i_d$ is the *d*-axis current error and $e_{iq} = i_{qref} - i_q$ is the *q*-axis current error. The decoupling terms $(-\omega_r L_q i_q)$ and $(\omega_r (L_d i_d + \lambda_m))$ are used in (15) and (16) respectively for the independent control of *d* and *q*-axis currents. The commanded *dq*-axis voltages (v_d, v_q) are transformed into *a, b, c* variables (v_a, v_b, v_c) and given to the PWM generator to generate the gate pulse for machine side converter.

5.4 Line Side Converter Control

The objective of the supply-side converter is to keep the DC-link voltage constant, regardless of the magnitude and direction of the rotor power. A vector control approach is used here, with the reference frame oriented along the stator (or supply) voltage vector position (Pena, 2001).

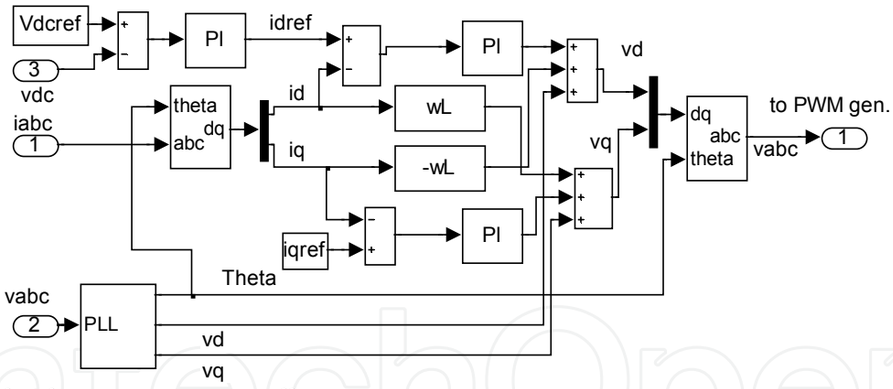

Fig. 8. Grid side converter controller.

Grid connected mode: The PQ control strategy with DC link voltage control is employed for grid connected operation of MTG system. In this scheme the power injected to the grid is regulated by controlling the injected current. The control structure for grid-connected mode operation of MTG system is shown in Figure 8. The standard PI-controllers are used to regulate the currents in the *dq* synchronous frame in the inner control loops as they have satisfactory behavior in regulating DC variables, as well as filtering and controlling can be easily achieved. Another PI controller is used in the outer loop to regulate the capacitor voltage in accordance with the current injected in to the grid. Its output is the reference for the active current PI controller. In order to obtain only a transfer of active power, the i_q current reference is set to zero. And also to have independent control of the current

components i_d and i_q the decoupling voltage components are added to the output of current PI controllers.
Converter voltages can be given as:

$$v_a(t) = \sqrt{\frac{2}{3}}\, V \cos(\omega t) \quad v_b(t) = \sqrt{\frac{2}{3}}\, V \cos(\omega t - \frac{2\pi}{3}) \quad v_c(t) = \sqrt{\frac{2}{3}}\, V \cos(\omega t - \frac{4\pi}{3}) \tag{17}$$

dq component in synchronous reference frame with decoupling terms can be represented as:

$$u_d = Ri_d + L_d \frac{di_d}{dt} + v_d - \omega L\, i_q \tag{18}$$

$$u_q = R\, i_q + L_q \frac{di_q}{dt} + \omega L_d i_d + v_q \tag{19}$$

Where, the dq currents are controlled by means of the right choice of the dq converter side voltages. Two PI regulators are command a PWM modulator to generate the voltage that should control the current.

Islanding mode: The islanding mode operation of single shaft MTG system requires a control different from that of grid connected mode. In this mode, the system has already been disconnected from the utility. Therefore the voltage and frequency is no longer regulated by it. Thus the output voltages are to be controlled in terms of amplitude and frequency which leads to control of the reactive and active power flow.

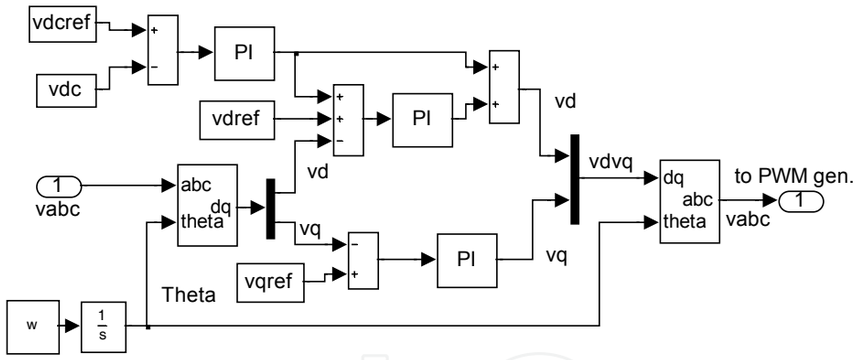

Fig. 9. Control structure for islanding mode operation

This is done by controlling the amplitude and frequency of the modulating input-signal to the PWM inverter. The control structure for islanding mode is depicted in Fig. 9. It consists of output voltage and DC link voltage PI controllers. The output voltage controllers control the output voltage with a minimal influence from nature of the load currents or load transients. A standard PI controller operating in the synchronously rotating coordinate system where, v_q is kept to zero is used. The DC voltage PI controller controls the DC voltage level based on the reference. For fast response the output of the DC voltage controller is feed forwarded to the voltage controller output. The DC link voltage controller acts only when the DC link voltage is below the reference and it lowers the voltage reference of the main voltage controller in order to avoid inverter saturation. The frequency control is done by integrating the constant reference frequency ω and using it for coordinate transfer of the voltage components from *abc* to *dq* and vice versa. In islanding mode, when there is

more generation than the load demand the DC link voltage becomes higher than the reference. .For this case damping chopper control is implemented. By activating this control excess energy stored in the Dc –link is dissipated in the damping resistor and hence maintain the Dc link voltage constant (Teodorescu, 2004). A proportional controller is used to control the duty cycle of the chopper. In practice, batteries are used to sore the excess energy.

One of the important requirements in the interconnection design of the power electronic converter interfaced DG system is that of synchronization to the utility system. (Chung, 2000) Synchronism of converter control with the grid is achieved by using a PLL. The Simulink block diagram of the PLL used in this work is shown in Fig. 10, where γ is the grid phase angle, v_x and v_y are the grid voltage components in the stationary reference frame. The philosophy of the PLL is that the sine of the difference between grid phase angle γ and inverter phase angle θ can be reduced to zero using a PI-controller, thus locking the inverter phase to the grid with small arguments ($\sin(\gamma-\theta) \cong (\gamma-\theta) = \Delta\theta$). The output of the PI controller is the inverter output frequency that is integrated to obtain the inverter phase angle θ. In order to improve the dynamic response at startup, the nominal frequency of the grid, ω_o is feed forwarded to the output of the PI controller. The major disadvantage of the three phase PLL is its sensitivity to grid voltage unbalance. Some attempts are made to extend this method for unbalanced voltages based on Symmetrical components (Ghartemani, 2004).

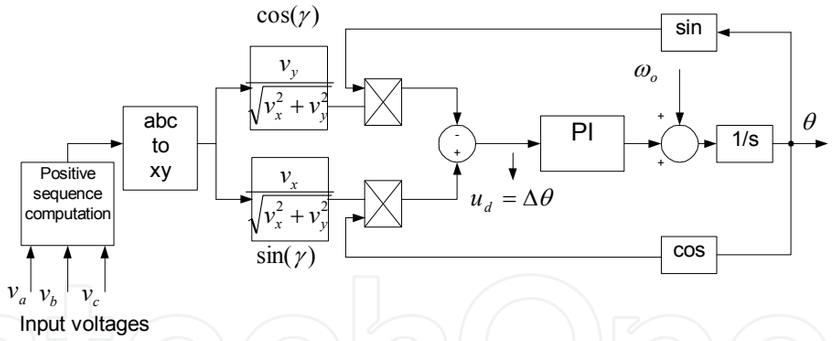

Fig. 10. PLL implemented in the Simulink

6. Simulation and Results

Figure 11 shows the simulation model implemented in the SimPowerSystems of the MATLAB to study the performance of the MTG system operation in grid connected mode (Gaonkar, 2008). The utility network, to which the MTG system is connected, is represented by a 3 phase sinusoidal source with its impedance. The series RL filter is used at the grid side of the MTG system. The simulation parameters of the model are given in Table 1. The micro turbine generation system takes per unit speed of the PMSM as input. The torque output of the microturbine is given as an input mechanical torque (T_m) to the PMSM. The direction of the torque T_m, is positive during motoring mode and made negative during generating mode of the PMSM. The machine side converter controller takes the rotor angle

speed and 3 phase stator current signals of the PMSM as inputs. In all the presented cases the voltage across the capacitor is zero, at the starting of simulation. During the start up, the PMSM operates as a motor to bring the turbine to a speed of 30,000 rpm. In this case power flows from the grid to MTG system.

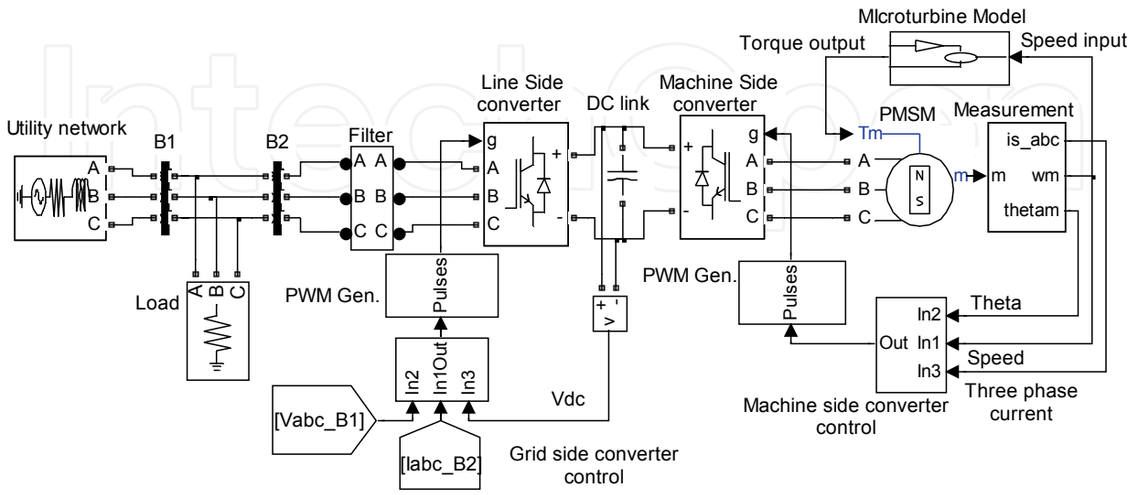

Fig. 11. Matlab/ SimPowerSystems implementation of MTG system connected to grid.

Grid parameters	480V, 60Hz, R_s=0.4Ωand L_s=2mH
Filter Parameters	L=0.97mH, R=0.21Ω
Switching Frequency	Grid side converter = 8 Khz
	Machine side Converter = 20 KHz
DC link capacitance	5000 µF
PI controllers sampling time	100 µsec
PMSM parameters	480 V, 30 kW ,1.6 KHz, 96000 rpm
	R_s=0.25 Ω, L_q=L_d=0.0006875 H
Microturbine parameters	Gain(K)=25,X=0.4,Y=0.05 and Z=1

Table 1.Simulation parameters for the model shown in Fig. 11

Figure 12 shows that the microturbine reaches the set value of speed in 0.4 sec. At this speed, the MTG system absorbs power of 5.4 kW as shown in Fig. 12 (b). The PMSM terminal voltage reaches 192 V at a frequency of 500 Hz at this speed. To ensure this operating condition at an unity displacement factor, the pre-calculated reference speed and direct current component i_d are set to 3142 rad/s and -5.36 A respectively (Morimoto, 1994). The speed regulator provides the reference for the i_q current component. At t=0.4 sec, the sign of the PMSM input torque is changed to operate it in generating mode. The power starts flowing from the MTG system to grid as shown in Fig. 12 (b).

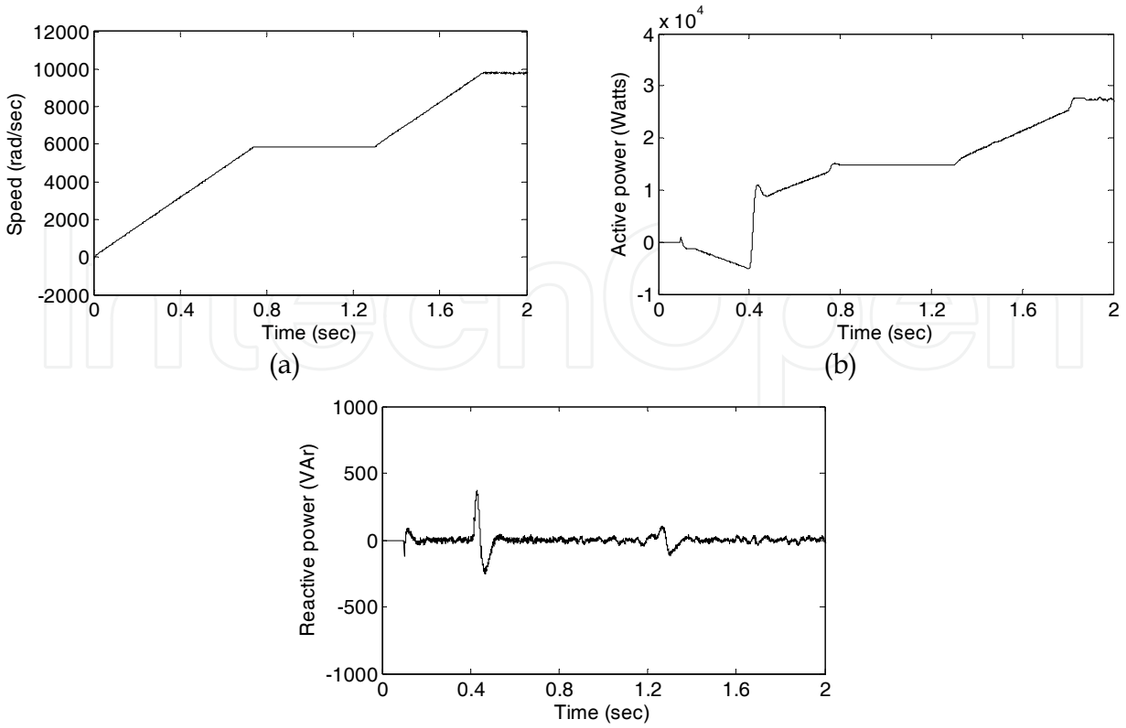

Fig. 12. Motoring and generating operation of PMSM (a) speed variation of PMSM (b) active power variation at the grid side of the MTG system (c) reactive power variations at the grid side of the MTG system.

At t=0.4 sec, the reference speed and i_d current are set to the pre-calculated values of 5849 rad/sec and -15.89 amps in order to generate power of 14 kW. In order to study the performance of the MTG system model for the change in power, the reference values of speed and i_d current component are again changed at t=1.3 sec to generate the rated power of 28 kW. When PMSM generates 28 kW, its line to line voltage and fundamental RMS output current reach the value of 480 V and 33.84 A respectively. Fig. 12 (c) shows that the reactive power injected to the grid during the simulation period is zero.

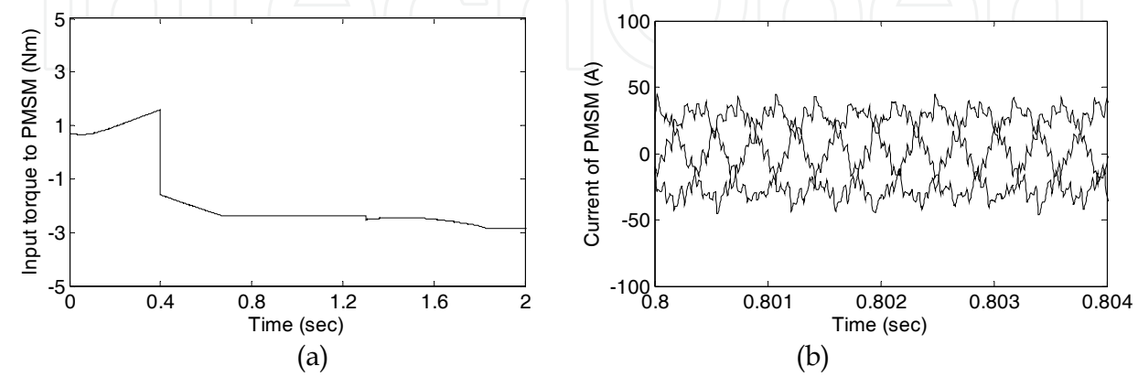

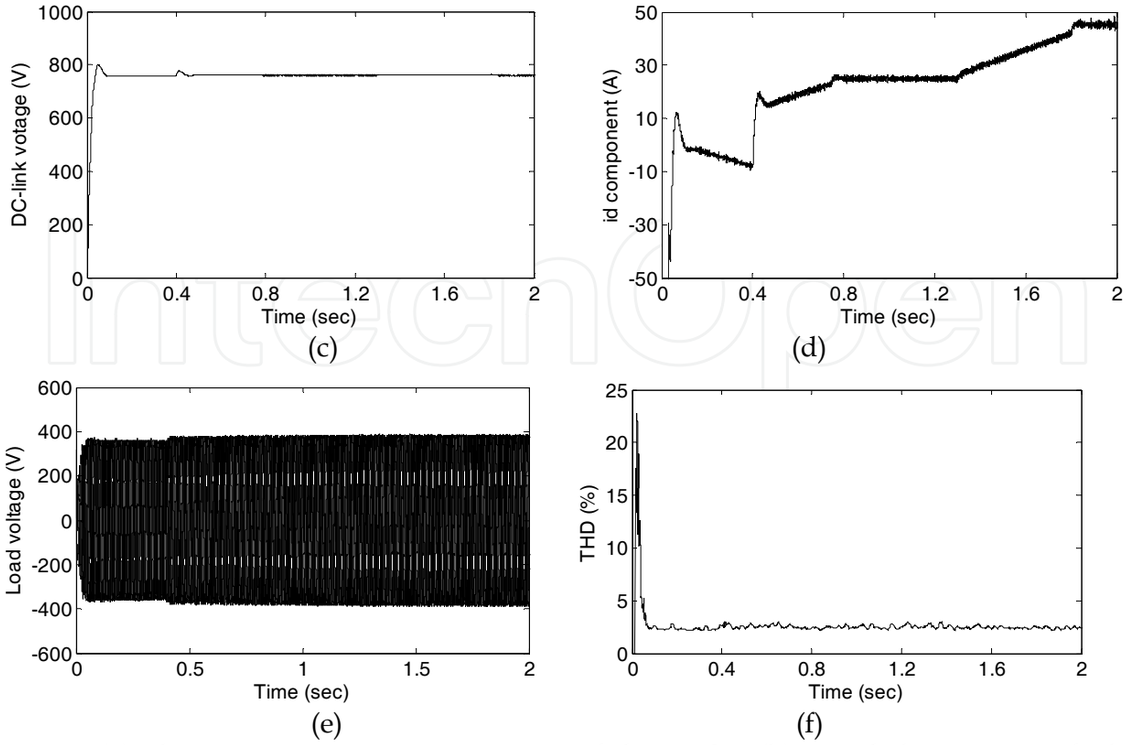

Fig. 13. (a) Electromagnetic torque variations of the PMSM (b) Detailed variations of the stator current of PMSM (c) DC link voltage variation (d) i_d component of the injected grid current (e) Line to line voltage at the load terminals (f) %THD variation at the load terminals.

Figure 13 (a) shows the variation of electromagnetic torque of the PMSM. In this it can be observed that, the change in the operation mode of PMSM in simulation is instantaneous. But this may not be the same in practical because of the inertia of the machine. Figure 13 (b) shows the nature of the stator current waveform of the PMSM. It can be observed from Fig. 13 (c) that the DC link voltage is regulated to 760 V by the grid side converter. Figures 13 (d) and (e) show the variation of i_d component of the injected grid current and the voltage across the terminals of the load. There is a small decrease in the voltage for t< 0.4 sec, as shown in Fig. 13 (e). This is due to the increasing power drawn by the MTG system during motoring mode operation as shown in Fig. 12 (b). In motoring mode both MTG system and load draw power from the grid. The total harmonic distortion (THD) of the voltage is about 2.3% during the entire simulation time as shown in Fig. 13 (f).

6.1 Response of the MTG model for various disturbances in the grid

Simulations are carried out to study the performance of developed the model of the MTG system under various disturbances originating from the grid. Three grid disturbance conditions are considered for study. They are balanced voltage dip, unbalanced voltage and harmonic distortion in the grid voltage. In all these conditions the MTG system is operated to deliver 28 kW.

Balanced voltage dips: The simulation results in Fig. 14 show the performance of the MTG system under balanced grid voltage dip. At t =1.4 to 1.5 sec (10 cycle), 20% balanced voltage

dip is introduced in the grid as seen from Fig. 14 (a). The variation of the injected reactive power due to the balanced dip is regulated to zero, by the grid side converter controller as shown in Fig. 14 (b). Figure(s) 14 (c), (d) and (e) show the variation in the active power output of the MTG system and i_q, i_d component of the injected current to the grid respectively.

Voltage unbalance: At t=1.4 sec the voltage unbalance in the grid is introduced by creating short circuit fault between phase A and ground. Thus the phase A voltage is reduced by 20% of its nominal value. In this case it is assumed that unbalance exist till the end of the simulation time. The simulated phase voltage of the grid is shown in Fig. 15 (a).

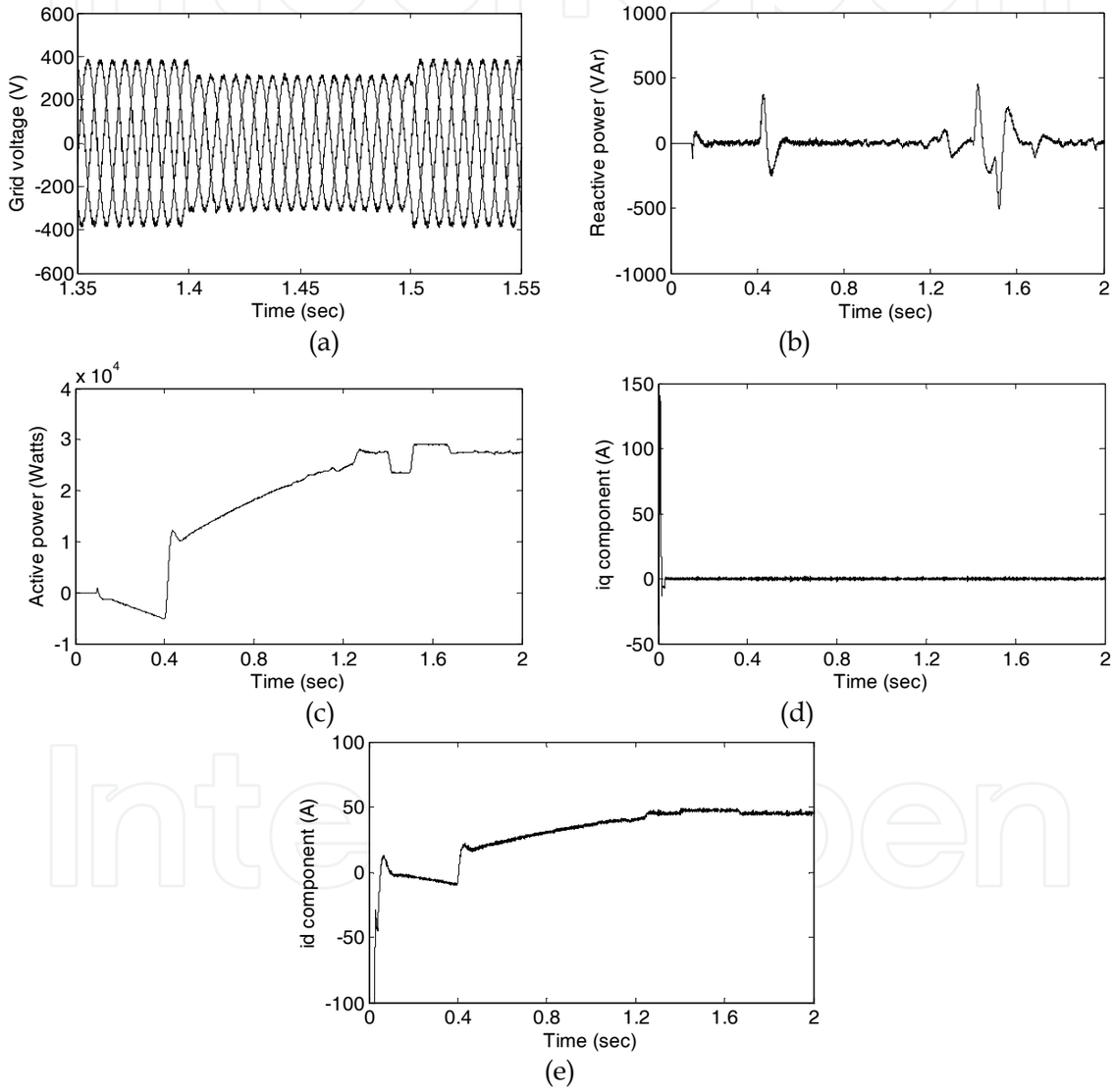

Fig. 14. Response of MTG system for balanced voltage dip in the grid. (a) balanced voltage dip in line to line grid voltage. (b) reactive power exchanged with grid (c) the injected active power to the grid. (d) i_q component of the injected current (e) i_d component of the injected current to the grid.

At the point of voltage unbalance, reactive power injected to the grid suddenly increases and then is regulated to zero as seen in Fig. 15 (b). The active power injected to the grid is not affected by the unbalance in the grid voltage as observed in Fig. 15 (c). There is no variation in the i_d and i_q components of the injected grid current during unbalance in the grid voltage as shown in Fig. 15 (d) and (e).During this unbalance phase A current increases to keep the active power output of the MTG system to constant.

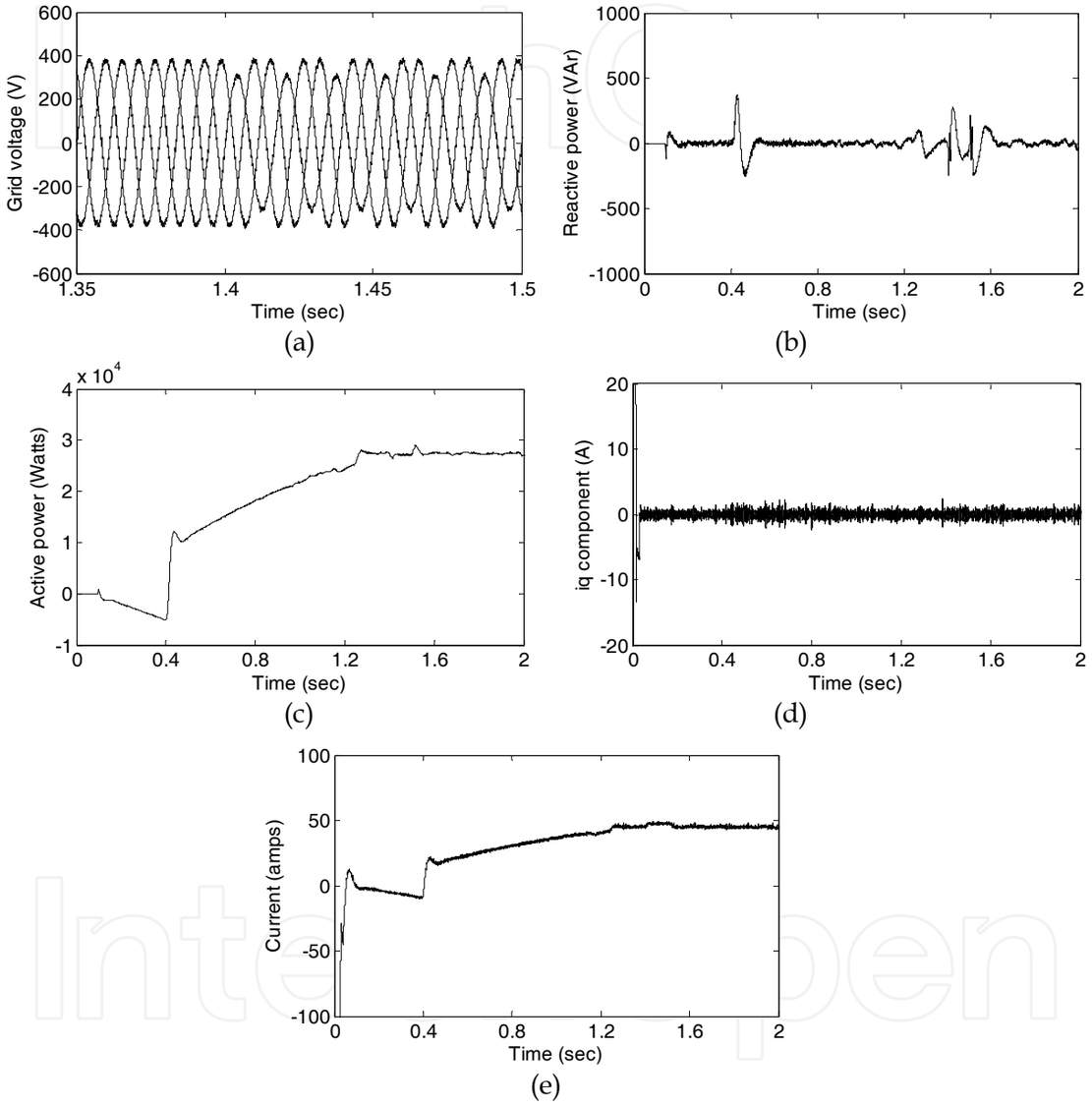

Fig. 15. Response of MTG system for voltage unbalances in the grid. (a)Unbalanced phase voltage of the grid (b) variation of injected reactive power to the grid (c) variations of injected active power to the grid (d) i_q component of the injected current to the grid (e) i_d component of the injected current to the grid.

Polluted grid voltage: The simulation results in Fig. 16 show the performance of the MTG system under harmonic polluted grid voltages. The various non linear loads connected to the grid are the main cause for the harmonic pollution in the grid voltage. In order to study

the performance of the model under polluted grid voltage, along with the fundamental component 10% of 5th and 6% of 7th harmonics are injected to the grid. The polluted grid voltages under this condition are shown in Fig. 16 (a). As per IEEE Standard 1547-2003 (IEEE, 2003), the THD at the point of common coupling to the grid should be kept below 5% but in this case it varies from 10% to 8% as shown in Fig. 16 (b) Fig. (s) 16 (c) and (d) show the variation of reactive power exchanged with the grid and injected active power respectively. The variation of the *dq* component of the injected line currents is shown in Fig. 16 (e) and (f) respectively.

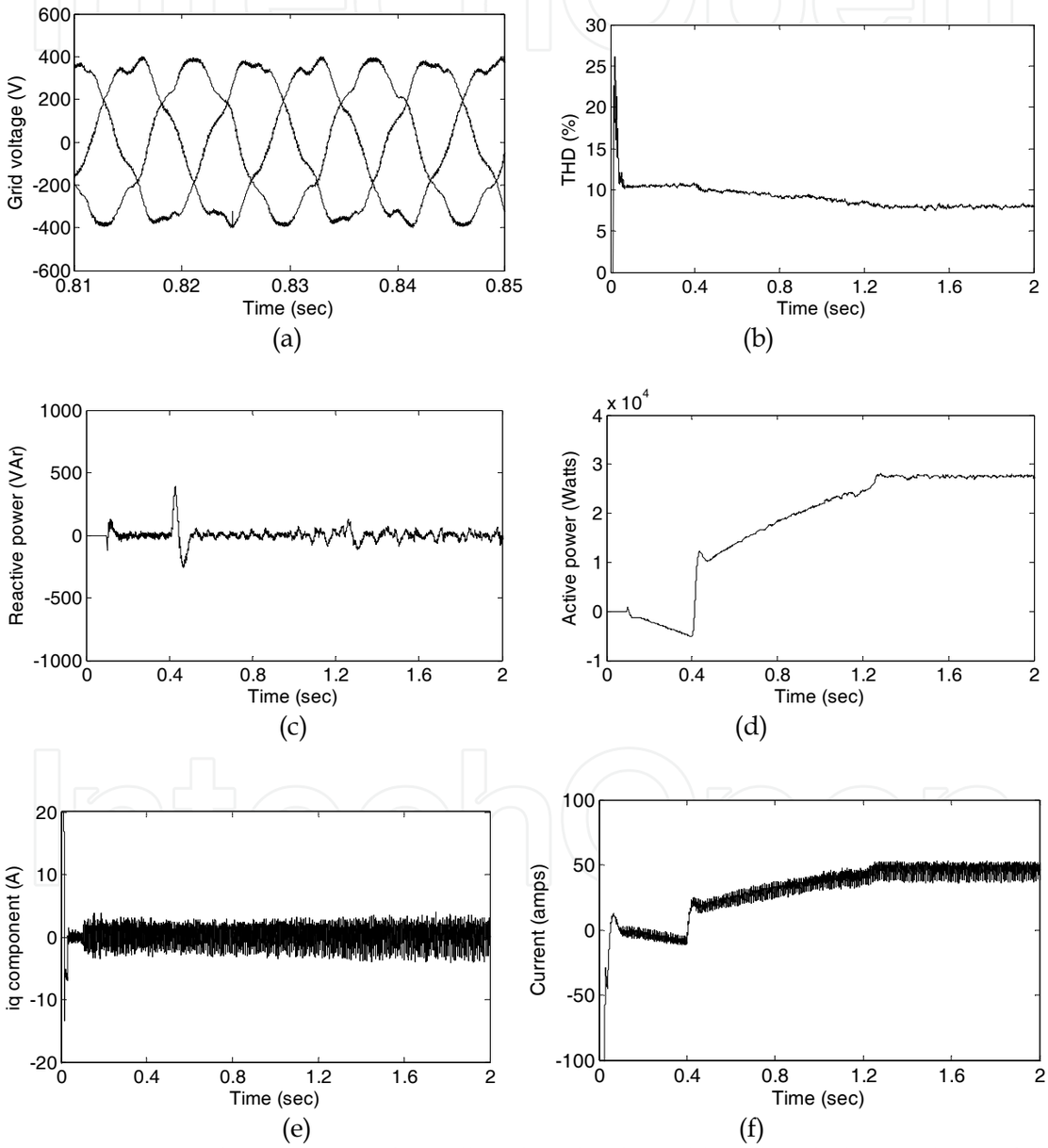

Fig. 16. Response of MTG system for polluted grid voltage (a) polluted phase voltage of the grid (b) variation of the THD in percentage (c) variation of injected reactive power to the

grid (d) variations in injected active power to the grid (e) i_q component of the injected current to the grid (f) i_d component of the injected current to the grid.

6.2 Seamless Transfer Scheme

The scheme consists of passive islanding detection and re-closure method. The presented islanding detection method uses the phase angle estimated by PLL to detect the islanding condition (Gaonkar, 2009). The re-closure scheme continuously monitors the phase angle and terminal voltage magnitude to determine whether disturbance in the grid is over or not. This is necessary in order to synchronize the MTG system and to connect back to grid, without any down time. The PLL block used in inverter control is employed for this scheme, hence no additional hardware needed. The structure of the PLL used to determine the phase angle error required by the proposed scheme has been described in the section 5.4.

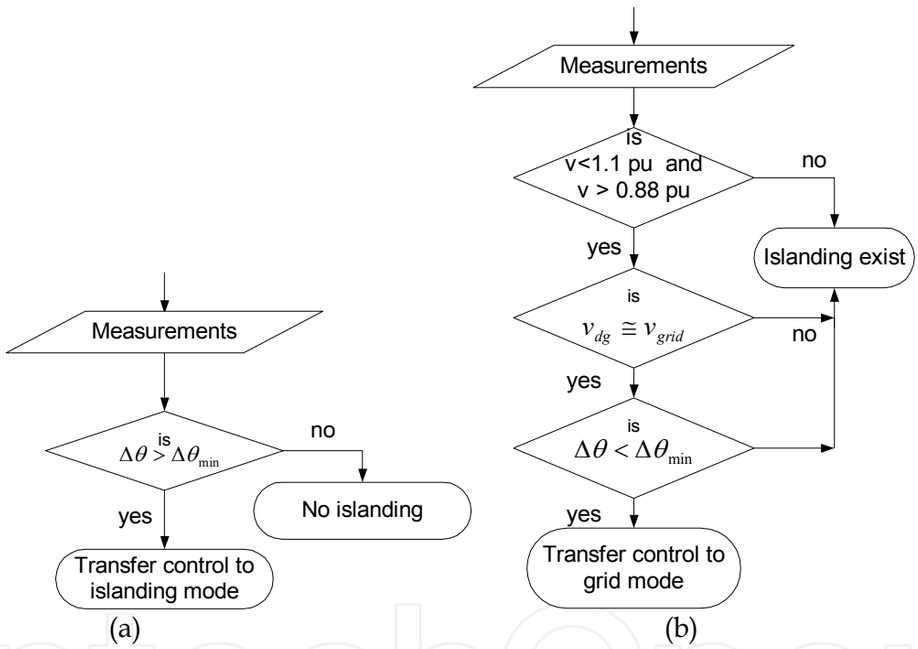

Fig. 17. (a) Islanding detection scheme (b) Re-closure scheme

Once the voltages are approximately equal then algorithm compares the $\Delta\theta$ value obtained from PLL with the set threshold limit. As long as these minimum requirements are met (voltage and phase), there are no major issues hindering the reconnection of islanded systems to the utility without de-energizing and causing downtimes.

Islanding Detection and Re-closure Method: The algorithm devised for the detection scheme is shown in Fig. 17 (Gaonkar 2009). The algorithm compares the phase angle error ($\Delta\theta$) obtained from the PLL, with that of the threshold value. If $\Delta\theta$ exceeds the set threshold limit, then islanding is confirmed. At the same time control of the inverter is transferred from the current control mode (grid connected) to voltage control mode (islanding mode). During the grid connected mode $\Delta\theta$ is approximately zero. Once the grid fails, phase angle error starts to increase. The $\Delta\theta$ value is obtained by PLL as explained in

section 5.4. This algorithm gives accurate results even under matching load conditions. The re-closure algorithm for connecting MTG system to grid, when utility recovers from the disturbance is shown in Fig. 17. The two main obstacles in implementing this type of re-closure are matching voltage magnitude and phase angle between converter and the grid. If this is not done, large transient will take place which will damage the MTG system. The re-closure algorithm continuously monitors terminal voltage of the grid and MTG system. Both voltage magnitudes are compared. As per IEEE std.1547-2003 DG terminal voltage should be in between 1.1 and 0.88 per unit of the nominal voltage. Both the voltage should be approximately equal, to avoid large transients during re-connection to grid.

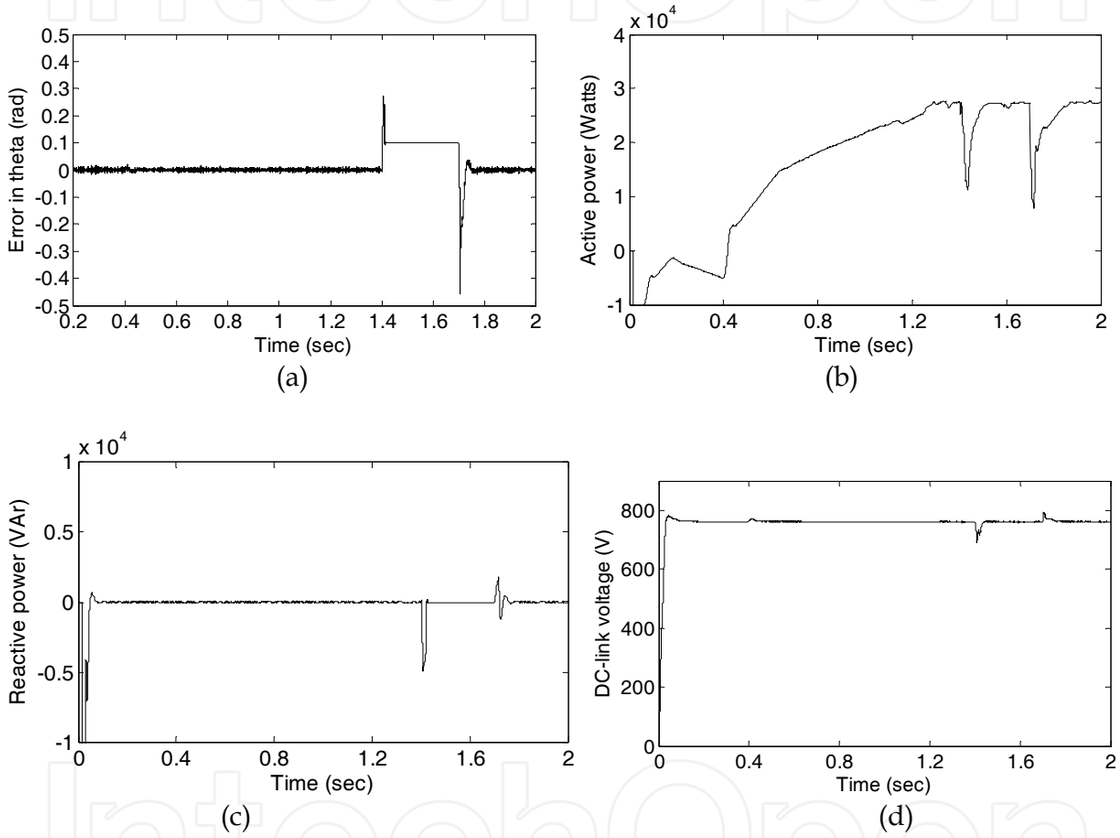

Fig. 18. (a) Phase angle error ($\Delta\theta$) variation (b) active power injected to the grid by MTG system (c) reactive power exchanged with the grid (d) DC link voltage

Utility Interactive to Islanding Mode: The MTG system acts as a motor during starting to launch the microturbine. Once microturbine reaches the speed of 3142 rad/sec at t=0.4 sec, the PMSM is operated as generator by changing the direction of its input torque to negative. During generating mode power flows from MTG system to grid. The phase angle error between the grid voltage and converter voltage is approximately zero as shown in Fig. 18 (a). In grid connected mode MTG system is operated to inject 28 kW as shown in Fig. 18 (b). The other parameters variations during this mode of operation are given in Fig(s). 18 (c) and (d). At t=1.4 sec, utility connection to the DG is disconnected by opening the circuit breaker.

This results in formation of a planned islanding situation comprising local load and MTG system. Opening of the circuit breaker can occur due to the faults and other grid disturbances. When the circuit breaker is opened, the phase angle difference ($\Delta\theta$) between grid voltage and the inverter voltage obtained from PLL starts to increase. The islanding detection algorithm given in Fig. 17 continuously monitors the $\Delta\theta$ variation. Once $\Delta\theta$ crosses the threshold limit of 0.08 *rad* then islanding is detected and converter control switches to islanding mode. The algorithms detect the islanding condition and transfer the control almost instantaneously. The variation of $\Delta\theta$, active power, reactive power and i_d component of the injected grid current are shown respectively in Fig (s). 18 (a), (b), (c) and (d). During this transition dip in DC link voltage can be observed from Fig. 18 (d).This is due to the variation in active power output of the MTG system. During the islanding mode MTG system supplies the power requirement of the load. Hence current supplied by the utility is zero as observed from Fig. 19 (a)

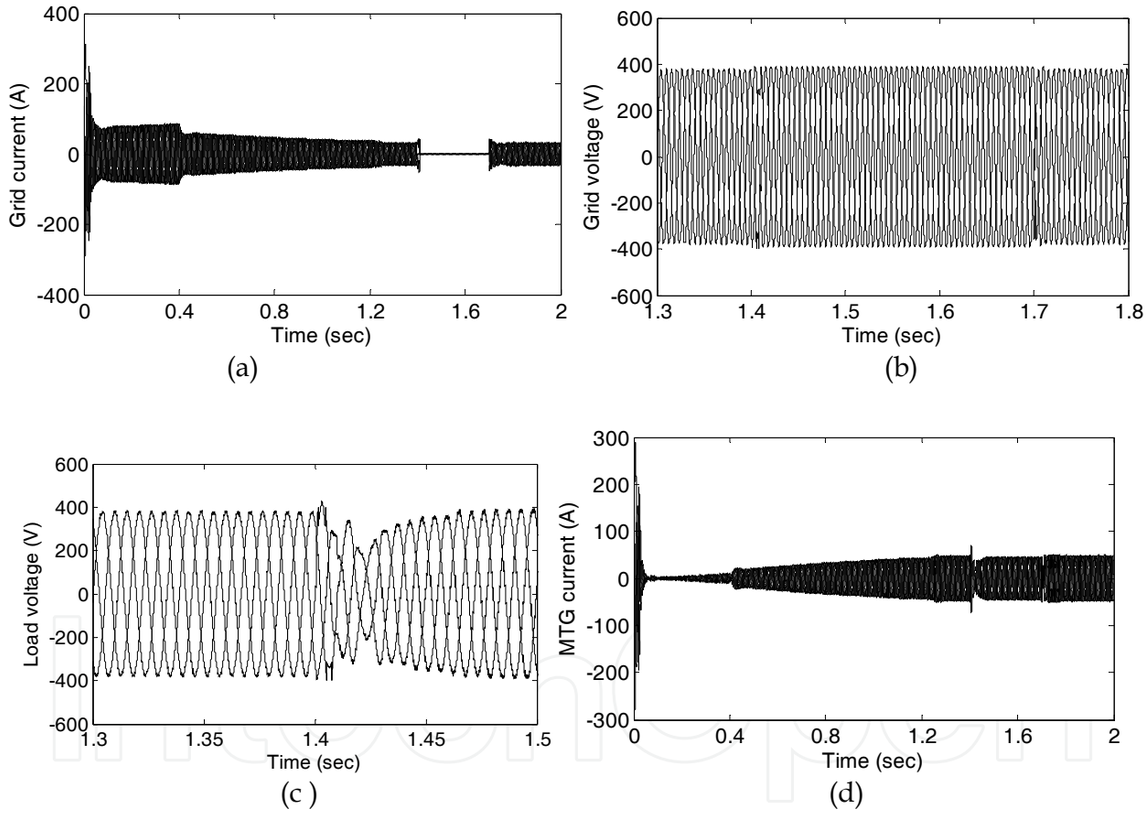

Fig. 19. (a) Line current of the grid (b)phase voltage of the grid (c)detailed variation of load phase voltage (d)line current at the grid side of MTG system

Islanding To Utility Interactive Mode: At t= 1.7 sec, the synchronization process starts to reconnect the DG to utility. The re-closure algorithm compares the grid voltage magnitude and phase angle with the MTG systems terminal voltage and phase angle. When the utility voltage magnitude approximately matches with that of MTG system and $\Delta\theta$ is less than the threshold then DG is connected to the utility. During this transition variation of $\Delta\theta$, active

power, reactive power, i_d component of the injected grid current and DC link voltage are shown respectively in Fig(s). 4.8 (a), (b), (c), (d) and (e). The variation of the line current of the grid, phase voltage and current variation of the MTG System terminals are shown in Fig.19.

7. Conclusion

The Distributed generation based on microturbine technology is new and a fast growing business. These DG systems are quickly becoming an energy management solution that saves money, resources, and environment in one compact and scalable package- be it stationary or mobile, remote or interconnected with the utility grid. In this thesis the MTG system model suitable for grid connected and islanding operation has been presented.The detailed modeling of a single-shaft MTG system suitable for grid connection and islanding operation has been developed in Simulink of the Matlab and is described in this chapter. The developed model allows the bidirectional power flow between grid and MTG system, hence need of extra converter for starting and shut down operation of MTG system can be avoided. The multi-loop control structure with decoupling terms used for grid and machine side converters has better performance. The three phase PLL structure described in this chapter uses only positive sequence component of the voltage. Hence gives accurate estimation of the phase angle even under grid disturbance conditions. A seamless transfer scheme for MTG system operation between grid connected and intentional islanding mode has been proposed in this chapter. The presented automatic mode switching scheme helps in providing continuous power supply to the customer even during outages of the utility and. is simple to implement without any additional hardware. The model shows good performance in both grid connected and islanding mode of operations. Thus the developed model of MTG system can be used as a tool suitable for studying and for performing accurate analysis of most electrical phenomena that occur when a microturbine is connected to the grid. As the issues are new and are the key for sustainable future power supply, lot of research is required to study their impacts and exploit them to the full extent.

8. References

Al-Hinai, A., and Feliachi, A., (2002), Dynamic model of microturbine used as a distributed generator, *Proceedings of the 34th South Eastern Symposium on System Theory*, ,pp. 209–213, 18–19 March 2002, Huntsville, AL.

Azmy, A. M., and Erlich, I., (2003), Dynamic simulation of fuel cells and microturbines integrated with a multi-machine network," *Proceedings of the IEEE Bologna Power Tech Conference*, Vol. 2, pp. 2212–2219, Bologna, Italy.

Barsali, S., Ceraolo, M., Pelacchi, P., and Poli, D., (2002), Control techniques of dispersed generators to improve the continuity of electricity supply, *Proceedings of the IEEE PES Winter Meeting*,Vol. 2, pp. 27–31, 2002.

Capstone Microturbine Documentation, Available at : www.capstoneturbine.com

Chung, S.-K., (2000), Phase-locked loop for grid-connected three-phase power conversion systems, *Proc. Inst. Elect. Eng.*, Vol. 147, No. 3, pp. 213–219, 2000.

Fethi, O., Dessaint, L. A., and Al-Haddad, K., (2004), Modeling and simulation of the electric part of a grid connected micro turbine, *Proceedings of the IEEE PES General Meeting*, Vol. 2, pp. 2212–2219, 2004.

Gaonkar, D. N., and Patel, R. N., (2006), Modeling and simulation of microturbine based distributed generation system, *Proceedings of the IEEE Power India Conference*, pp. 256–260, 10–12 April 2006. New Delhi, India,

Gaonkar, D. N., Pillai, G. N., and Patel, R. N., (2008), Dynamic performance of microturbine generation system connected to grid, *Journal of Elect. Power Compon. Syst.,* Vol. 36, No. 10, pp. 1031–1047, 2008.

Gaonkar, D. N., Pillai, G. N., and Patel, R. N., (2009), Seamless transfer of microturbine generation system operation between grid connected and islanding modes, *Journal of Elect. Power Compon. Syst.,* Vol. 37, No. 10, pp. 174–188, 2009.

Ghartemani, M. K., and Iravani, M. R., (2004), A method for synchronization of power electronic converters in polluted and variable frequency environment, IEEE Trans. Power Syst., Vol. 19,No. 3, pp. 1263–1270, 2004.

Guda S. R., Wang C. and Nehrir M. H., (2004), Modeling of microturbine power generation systems, *Electrical Power System and Components*, vol. 34, no. 9, pp. 1027–1041.

Hajagos, L. M., and Berube, G. R., (2001), Utility experience with gas turbine testing and modelling, *Proc. IEEE PES Winter Mtg*., Vol. 2, pp. 671–677, 2001.

IEEE, (2003), IEEE standard for interconnecting distributed resources with electric power systems, IEEE Std. 1547-2003, 2003.

Illinda, M., and Venkatramanan, G. (2002), Control of distributed generation systems to mitigate load and line imbalances, *Proceedings of the IEEE Electronics and Specialists Conference*, Vol. 4, pp. 2013–2201, 2002.

Morimoto, S., Sanada,M., and Takeda,Y., (1994), Wide speed operation of interior permanent magnet synchronousmotors with high performance current regulator, *IEEE Trans. Indl. Appl*., Vol. 30, pp. 920–926, 1994.

Nikkhajoei, H., and Iravani, R., (2005), A matrix converter based microturbine distributed generation system, *IEEE Trans. Power Delivery*, Vol. 20, No. 3, pp. 2182–2192, 2005.

Pillai, P., and Krishnan, R., (1989), Modeling, simulation, and analysis of permanent-magnet motor drives, Part I: The permanent-magnet synchronous motor drive, *IEEE Trans. Indl. Appl.,*Vol. 25, No. 2, pp. 265–273, 1989.

Pena, R. Cardenas, R. Blasco R., G. Asher G. and J. Clare J., (2001), A cage induction generator using back-to-back PWM converters for variable speed grid connected wind energy system," in *Proc. IECON'01 Conf.*, vol. 2, 2001, pp. 1376–1381,2001.

Rowen, W. I., (1983), Simplified mathematical representations of heavy duty gas turbines, *ASME Trans. J. Eng. Power*, Vol. 105, No. 4, pp. 865–869, 1983.

Scott, W. G., (1998) , Microturbine generators for distribution systems, *IEEE Industry Appl. Mag*.,Vol. 4, No. 3, pp. 57–62,1998.

Teodorescu, R., and Blaabjerg, F., (2004), Flexible control of small wind turbines with grid failure detection operating in stand-alone and grid-connected mode, *IEEE Trans. Power Electronics*.,Vol. 19, No. 5, pp. 1323–1332, 2004.

Tirumala, R., Mohan, N., and Henze, C., 2002, Seamless transfer of grid-connected PWM inverters between utility-interactive and stand-alone modes, *Proc. 17th Ann. IEEE Appl. Power Electron. Conf. Exposit*., Vol. 2, pp. 1081–1086, 2002.

Villeneuve, P. L., 2004, Concern generated by islanding, *IEEE Power Energy Mag.*, Vol. 2, No. 3, pp. 49–53, 2004.

Distributed Generation

Edited by D N Gaonkar

ISBN 978-953-307-046-9
Hard cover, 406 pages
Publisher InTech
Published online 01, February, 2010
Published in print edition February, 2010

In the recent years the electrical power utilities have undergone rapid restructuring process worldwide. Indeed, with deregulation, advancement in technologies and concern about the environmental impacts, competition is particularly fostered in the generation side, thus allowing increased interconnection of generating units to the utility networks. These generating sources are called distributed generators (DG) and defined as the plant which is directly connected to distribution network and is not centrally planned and dispatched. These are also called embedded or dispersed generation units. The rating of the DG systems can vary between few kW to as high as 100 MW. Various new types of distributed generator systems, such as microturbines and fuel cells in addition to the more traditional solar and wind power are creating significant new opportunities for the integration of diverse DG systems to the utility. Interconnection of these generators will offer a number of benefits such as improved reliability, power quality, efficiency, alleviation of system constraints along with the environmental benefits. Unlike centralized power plants, the DG units are directly connected to the distribution system; most often at the customer end. The existing distribution networks are designed and operated in radial configuration with unidirectional power flow from centralized generating station to customers. The increase in interconnection of DG to utility networks can lead to reverse power flow violating fundamental assumption in their design. This creates complexity in operation and control of existing distribution networks and offers many technical challenges for successful introduction of DG systems. Some of the technical issues are islanding of DG, voltage regulation, protection and stability of the network. Some of the solutions to these problems include designing standard interface control for individual DG systems by taking care of their diverse characteristics, finding new ways to/or install and control these DG systems and finding new design for distribution system. DG has much potential to improve distribution system performance. The use of DG strongly contributes to a clean, reliable and cost effective energy for future. This book deals with several aspects of the DG systems such as benefits, issues, technology interconnected operation, performance studies, planning and design. Several authors have contributed to this book aiming to benefit students, researchers, academics, policy makers and professionals. We are indebted to all the people who either directly or indirectly contributed towards the publication of this book.

How to reference

In order to correctly reference this scholarly work, feel free to copy and paste the following:

Dattatraya N. Gaonkar (2010). Performance Of Microturbine Generation System in Grid Connected and Islanding Modes of Operation, Distributed Generation, D N Gaonkar (Ed.), ISBN: 978-953-307-046-9, InTech, Available from: http://www.intechopen.com/books/distributed-generation/performance-of-microturbine-generation-system-in-grid-connected-and-islanding-modes-of-operation

INTECH
open science | open minds

InTech Europe
University Campus STeP Ri
Slavka Krautzeka 83/A
51000 Rijeka, Croatia
Phone: +385 (51) 770 447
Fax: +385 (51) 686 166
www.intechopen.com

InTech China
Unit 405, Office Block, Hotel Equatorial Shanghai
No.65, Yan An Road (West), Shanghai, 200040, China
中国上海市延安西路65号上海国际贵都大饭店办公楼405单元
Phone: +86-21-62489820
Fax: +86-21-62489821

IntechOpen